International Journal of Cardiology 280 (2019) 152–159

Contents lists available at ScienceDirect

International Journal of Cardiology

journal homepage: www.elsevier.com/locate/ijcard

MicroRNA-26b relieves inflammatory response and myocardial remodeling of mice with myocardial infarction by suppression of MAPK pathway through binding to PTGS2

Zhen-Wei Ge [a,1], Xi-Liang Zhu [a,1], Bao-Cai Wang [a], Jun-Long Hu [a], Jun-Jie Sun [a], Sheng Wang [a], Xian-Jie Chen [a], Shu-Ping Meng [b], Lin Liu [c], Zhao-Yun Cheng [a,*]

[a] Department of Cardiovascular Surgery, Henan Provincial People's Hospital, Zhengzhou 450003, PR China
[b] ICU of Cardiovascular Surgery, Henan Provincial People's Hospital, Zhengzhou 450003, PR China
[c] Department of Cardiovascular Ultrasound, Henan Provincial People's Hospital, Zhengzhou 450003, PR China

ARTICLE INFO

Article history:
Received 23 July 2018
Received in revised form 19 December 2018
Accepted 27 December 2018
Available online 4 January 2019

Keywords:
MicroRNA-26b
PTGS2
MAPK pathway
Myocardial infarction
Inflammatory response
Myocardial remodeling

ABSTRACT

Background: Myocardial infarction (MI) is a common cardiovascular disease caused by myocardial ischemia. Also, microRNA (miRNA) participates in the pathophysiology of many cardiovascular diseases, which can affect stem cell transplantation in the treatment of MI. In this study, our aim is to explore effect of miR-26b on inflammatory response and myocardial remodeling through the MAPK pathway by targeting PTGS2 in mice with MI.
Methods: Microarray data analysis was conducted to screen MI-related differentially expressed gens (DEGs). Relationship between miR-26b and PTGS2 was testified. Cardiac function, inflammatory reaction, infarct size, and myocardial fibrosis were observed. The miR-26b expression and mRNA and protein levels of, PTGS2, ERK, JNK and p38 and Bcl-2/Bax were examined. The effect of miR-26b on cell apoptosis was also analyzed.
Results: MiR-26b was predicted to target PTGS2 further to mediate the MAPK pathway, thus affecting MI. MiR-26b negatively targeted PTGS2. MI mice showed decreased cardiac function, as well as increased inflammatory reaction, myocardial injury, area of fibrosis and myocardial cell apoptosis. After injection of miR-26b agomir or NS-398 (PTGS2 inhibitor), inflammatory response of MI mice was attenuated and myocardial remodeling induced by MI was alleviated.
Conclusion: These findings indicate that miR-26b inhibits PTGS2 to activate the MAPK pathway, so as to reduce inflammatory response and improve myocardial remodeling in mice with MI.

1. Background

Myocardial infarction (MI) is a kind of cardiovascular disease caused by imbalance of blood supply and abnormalities in cardiac vasomotion and dissection [1]. There are over 17 million deaths for cardiovascular disease every year and the annual mortality rate for patients with acute MI and impaired left ventricular function accounts for 13% [2]. Recently, such therapy for MI as using growth factors to enhance the heart's intrinsic capacity of reacting to acute damage has been developed [3]. Although certain progress in the treatment of MI has been made, a lot of patients die early with acute MI and those who survive are still in danger of developing heart failure, which indicates that current therapy for MI still lacks key pathophysiologic mechanisms [4]. There is therefore a need to develop new idea to study additional therapy for MI.

MicroRNA-26b (miR-26b) is a hypoxia regulated miRNA, and it was down-regulated in response to the exposure of hypoxia, where serum response factor was up-regulated in response to the exposure of hypoxia [5]. Besides, it has been found forced-expression of miR-26b attenuated cardiac hypertrophy and plasma miR-26b levels also down-regulated in acute heart failure patients [6], which indicated miR-26b played a significant role in cardiac function. Additionally, inhibition of miR-26a has been reported to rapidly induce angiogenesis and diminish acute MI size with enhanced heart function in a mouse model with acute MI [7]. miR-26a and miR-26b are reported to target the expression of prostaglandin-endoperoxide synthase 2 (PTGS2, also called as COX-2) to regulate allergic inflammation [8]. PTGS2 is a kind of enzyme in the transformation from arachidonic acid to prostaglandins which is capable of enhancing the neoplastic process by suppressing apoptosis, promoting proliferation and angiogenesis [9]. The expression of PTGS2 was induced by cytokines, oncogenes, and tumor promoters, and it was highly expressed in various cancers [10]. Also, it has been demonstrated that PTGS2 gene was related

* Corresponding author at: Department of Cardiovascular Surgery, Henan Provincial People's Hospital, No.7, Weiwu Road, Zhengzhou 450003, Henan Province, PR China.
E-mail address: czyczhaoyun@126.com (Z.-Y. Cheng).
[1] These authors contributed equally to this work.

https://doi.org/10.1016/j.ijcard.2018.12.077
0167-5273/

to a decreased risk of MI and stroke, which suggests important role of PTGS2 in therapy for MI [11]. Meanwhile, mitogen-activated protein kinase (MAPK) pathway contributed to regulation of cell viability, apoptosis and invasion *via* phosphorylating a number of substrates [12]. MAPK can function as potentially key regulatory elements in cardiac myocyte pathophysiology and affects expression of its target genes to lead to cellular response in different kinds of cardiac disease forms [13]. Accordingly, we may hypothesize that miR-26b displays influence on MI through MAPK pathway by regulating PTGS2.

2. Materials and methods

2.1. Ethics statement

This study was carried out in strict accordance with the recommendations of the Guide for the Care and Use of Laboratory Animals of the National Institutes of Health. The protocol was approved by Institutional Animal Care and Use Committee of our hospital.

2.2. Microarray-based analysis

In the Gene Expression Omnibus (GEO) database (https://www.ncbi.nlm.nih.gov/geo/), "myocardial infarction" was used as the key word to retrieve the gene chips of MI (Supplementary Table 1). GSE46395, GSE66360 and GSE97320 were employed for differentially expressed gene (DEG) screening. R language affy package [14] was used for background correction of gene expression data and standardized pretreatment and limma package [15] for DEG screening with p-value <0.05 and |LogFoldChange| > 2 as the threshold. The heatmap of DEG expression was drawn. TargetScan (http://www.targetscan.org/vert_71/), miRDB (http://www.mirdb.org/), miRSearch (http://www.exiqon.com/microrna-target-prediction), miRTarBase (http://mirtarbase.mbc.nctu.edu.tw/php/search.php) and microRNA.org (http://34.236.212.39/microrna/getGeneForm.do) were used to predict miRNA which could regulate DEGs. Custom Venn diagrams were calculated and drew with the Venn online analysis tool (http://bioinformatics.psb.ugent.be/webtools/Venn/) to compare the DEGs of three microarrays or 5 miRNA predictions.

2.3. Dual-luciferase reporter gene assay

Dual-luciferase reporter gene assay was performed according to a previous study [16]. After 48-h transfection, the cells were collected and lysed, and Dual-Luciferase® Reporter Assay System (Promega Corp., Madison, WI, USA) was used to conduct luciferase activity detection with a Luminometer TD-20/20 detector (E5311, Promega Corp., Madison, WI, USA). The experiment was conducted three times.

2.4. Establishment of mouse model of MI

Mouse model of MI was established [17]. The model establishment was considered successful when the anterior wall of left ventricular appeared pale and electrocardiograph showed that 0.2 mV ST segment elevation on more than two limb guide chains. The sham group was only conducted seton without ligating the coronary artery. Heart was immediately put into thorax after ligation and muscle and skin were sutured.

2.5. Experimental animals and grouping

Forty-eight male specific-pathogen-free (SPF) C57BL/6 mice (aged 8–10 weeks old; weighting 20–24 g; Beijing Vital River Laboratory Animal Technology Co., Ltd.) were used in this study. The mice were grouped into following six groups (eight mice each): sham group (conducting MI sham operation), MI group (MI model), MI + miR-26b agomir group (miR-26b mimic being injected into caudal vein after MI modeling), MI + miR-26b antagomir group (miR-26b inhibitor being injected into caudal vein after MI modeling), MI + NS-398 group (PTGS2 inhibitor being injected into caudal vein after MI modeling), and MI + miR-26b antagomir + NS-398 group (miR-26b inhibitor and NS-398 [PTGS2 inhibitor] being injected into caudal vein after MI modeling). These mice were granted with free access to ordinary feed and water, and it was ensured there were 12-h illumination time and darkness time respectively in the cage. The miR-26b agomir and miR-26b antagomir free-dried powder coated with cholesterol were dissolved into phosphate-buffered saline (PBS) to prepare suspension, 10 nmol of suspension and 5 mg/kg of NS-398 were respectively injected into caudal veins in 5 min and 3 days after modeling separately. Seven days after the MI model was established, the structure and cardiac function showed obvious change, then the small animal ultrasound system Vevo 770 (Visual Sonics Co., Toronto, Canada) was applied to measure cardiac function. Finally, the mice were sacrificed to collect the tissues for future experiments.

2.6. Echocardiography

Seven days after the MI modeling, cardiac function was evaluated by the Vevo 770 High-Resolution Imaging System (Visual sonic, Inc.). The left ventricular end-diastolic dimension (LVEDD), left ventricular end-systolic dimension (LVESD), left ventricular end-diastolic volume (LVEDV), and left ventricular end-systolic volume (LVESV) were measured and recorded. And the left ventricular ejection fraction (LVEF) and left ventricular fractional shortening (LVFS) were calculated according to following formulae: LVEF = [(LVEDV-LVESV) / LVEDV] × 100, LVFS = [(LVEDD-LVESD) / LVEDD] × 100. The mean values of three consecutive cardiac cycles were obtained [18,19].

2.7. Animal tissue sampling

On the first day and seventh day after the MI modeling, 400 μL of blood sample was taken from caudal veins of mice in each group and then allowed to stand at room temperature for 2 h. Expression of inflammatory factors was measured by enzyme-linked immunosorbent assay (ELISA). The above procedure was proceeded in the sham group at the same time. After the ultrasonic measurement, mice of each group were sacrificed by cervical dislocation. The heart was taken out immediately and myocardium from part of MI area was collected and frozen for reverse transcription quantitative chain reaction (RT-qPCR) and western blot analysis. The remaining myocardium was cut into 3-μm serial sections and used for hematoxylin-eosin (HE), Masson and TdT-mediated dUTP Nick-End Labeling (TUNEL) staining.

2.8. ELISA

Serum of mice from each group were collected for measurement of levels of tumor necrosis factor-α (TNF-α), interleukin-6 (IL-6) and interleukin-10 (IL-10). The experiment was conducted strictly according to instructions of ELISA kits (Abcam Inc., Cambridge, MA, USA). The universal ELISA instrument (Biotek Synergy 2) was employed to determine absorbance (A) at 450 nm of each well within 3 min to figure out target protein concentration of samples.

2.9. 2,3,5-Triphenylte-trazolium chloride (TTC) and HE staining

The heart was immediately taken out after mouse sacrifice and sliced into sections for TTC staining. The MI area appeared pale and non-MI area appeared erythrinus, and then Image J was employed to calculate percentage of MI area in ventricle area [19,20]. Five dewaxed sections above were taken and stained with hematoxylin for observation of morphological changes [21].

2.10. Masson staining

The five sections after dewaxing were selected for Masson staining [22]. The number of cells was counted in 10 randomly selected horizons to collect images, which were then analyzed with the Image J analysis software, and degree of myocardium fibrosis was expressed as percentage of fibrotic myocardium in total area of left ventricle.

2.11. RNA extraction and RT-qPCR

RNA extraction and RT-qPCR were conducted as recommended [23]. U6 was used as an internal reference for miR-26b and β-actin was used as an internal reference for other mRNA. The primer sequences are shown in Supplementary Table 2. The relative quantitative method was used to calculate and the 2-ΔΔCt was used to express the relative expression of target gene in each sample.

2.12. Western blot analysis

The Western blot analysis was performed based on a previous study [24]. The following primary rabbit anti-mouse polyclonal antibodies (diluted at 1: 1000) to PTGS2 (ab15191), p38 (phospho T180 + Y182; ab195049), ERK (ab54230), p-ERK (ab214036), JNK (ab179461), p-JNK (ab124956), Bax (ab32503), Bcl-2 (ab692), and GAPDH (ab181602) and secondary goat anti-rabbit polyclonal antibody to horseradish peroxidase-labeled IgG (ab20272, diluted at 1:500) were used. All antibodies were purchased from Abcam Inc. (Cambridge, MA, USA). The GAPDH was used as the internal reference, and the ratio of gray level between target band and internal control was quantified as the relative expression of protein. This experiment was repeated 3 times.

2.13. TUNEL staining

The selected five sections were stained. Ten views were randomly-selected from each section and the positive cells and myocardium cells were calculated with the average value obtained. The ratio of the tan nucleus and blue nucleus was quantified as the apoptotic index (AI) of myocardium cell [21].

2.14. Statistical analysis

Experimental data were analyzed using SPSS 18.0 software (SPSS Inc., Chicago, IL, USA). Measurement data are expressed as mean ± standard deviation, comparison among multiple groups was conducted by one-way analysis of variance and comparison between two groups was performed by t-test. $p < 0.05$ indicated statistical significance.

3. Results

3.1. MiR-26b is lowly expressed while PTGS2 enriched in MI

Using adjusted *p*-value <0.05 and |LogFoldChange| > 2 as the threshold, DEG analysis of MI was conducted using R language and 471, 351 and 455 DEGs were obtained from GSE46395, GSE66360 and GSE97320 chip, respectively. The top 100 genes of each chip were selected for comparison. Venn diagrams (Supplementary Fig. 1A) revealed an intersecting gene, PTGS2. The top 100 DEG heatmaps of GSE66360 (Supplementary Fig. 1B) and GSE97320 (Supplementary Fig. 1C) showed that the expression of PTGS2 in patients with MI was significantly higher than that in healthy controls. Through the expression of PTGS2 in GSE46395 chip (Supplementary Fig. 1D), we could see that the expression of PTGS2 in MI mouse model was significantly higher than that in the control group. Therefore, we focused on the significance and molecular mechanism of PTGS2 in MI. In order to further investigate the possible molecular mechanism of PTGS2, TargetScan, miRDB, miRSearch, miRTarBase and microRNA.org were employed to predict miRNAs related to PTGS2, which revealed 10, 42, 18, 3 and 40 potential miRNAs, respectively. Venn diagrams in each tools were drawn, with one miRNA, mmu-miR-26b-5p, found in the intersection (Supplementary Fig. 1E), indicating that miR-26b was most likely to regulate PTGS2. Furthermore, inhibition of the MAPK signaling pathway alleviates MI [25,26] and miR-26b inhibits the MAPK signaling pathway [11]. Combined with the microarray-based analysis, it could be concluded that miR-26b targets PTGS2 and mediates the MAPK signaling pathway in MI.

3.2. PTGS2 is a target gene of miR-26b

The target gene of miR-26b was analyzed according to the biology prediction website microRNA.org and it was testified that PTGS2 was the direct target gene of miR-26b (Supplementary Fig. 2A). The results showed that transfecting miR-26b mimic decreased the activity of luciferase reporter gene ($p < 0.05$) (Supplementary Fig. 2B), which indicated that miR-26b negatively targets PTGS2.

3.3. MiR-26b improves cardiac functions and relieves inflammatory response of mice with MI by downregulating PTGS2

To explore the effects of PTGS2 on cardiac functions in mice, we carried out follow-up studies by using NS-398, an inhibitor of PTGS2. LVEDD and LVESD of mice increased (Fig. 1A), LVFS and LVEF (Fig. 1B) of mice decreased in the MI group, the MI + miR-26b agomir group, the MI + miR-26b antagomir group, the MI + NS-398 group and the MI + miR-26b antagomir + NS-398 group than that in the sham group ($p < 0.05$). MI mice injected with miR-26b agomir and NS-398 had lower LVEDD and LVESD but higher LVFS and LVEF ($p < 0.05$), while MI mice injected with miR-26b antagomir had increased LVEDD and LVESD but decreased LVFS and LVEF ($p < 0.05$). These results suggested that up-regulation of miR-26b may reduce the effect of MI on cardiac functions by down-regulating the expression of PTGS2.

ELISA results showed that compared with the sham group, mice in the MI, MI + miR-26b agomir, MI + miR-26b antagomir, MI + NS-398 and MI + miR-26b antagomir + NS-398 groups had increased expression of TNF-α (Fig. 1C) and IL-6 (Fig. 1D) but decreased expression

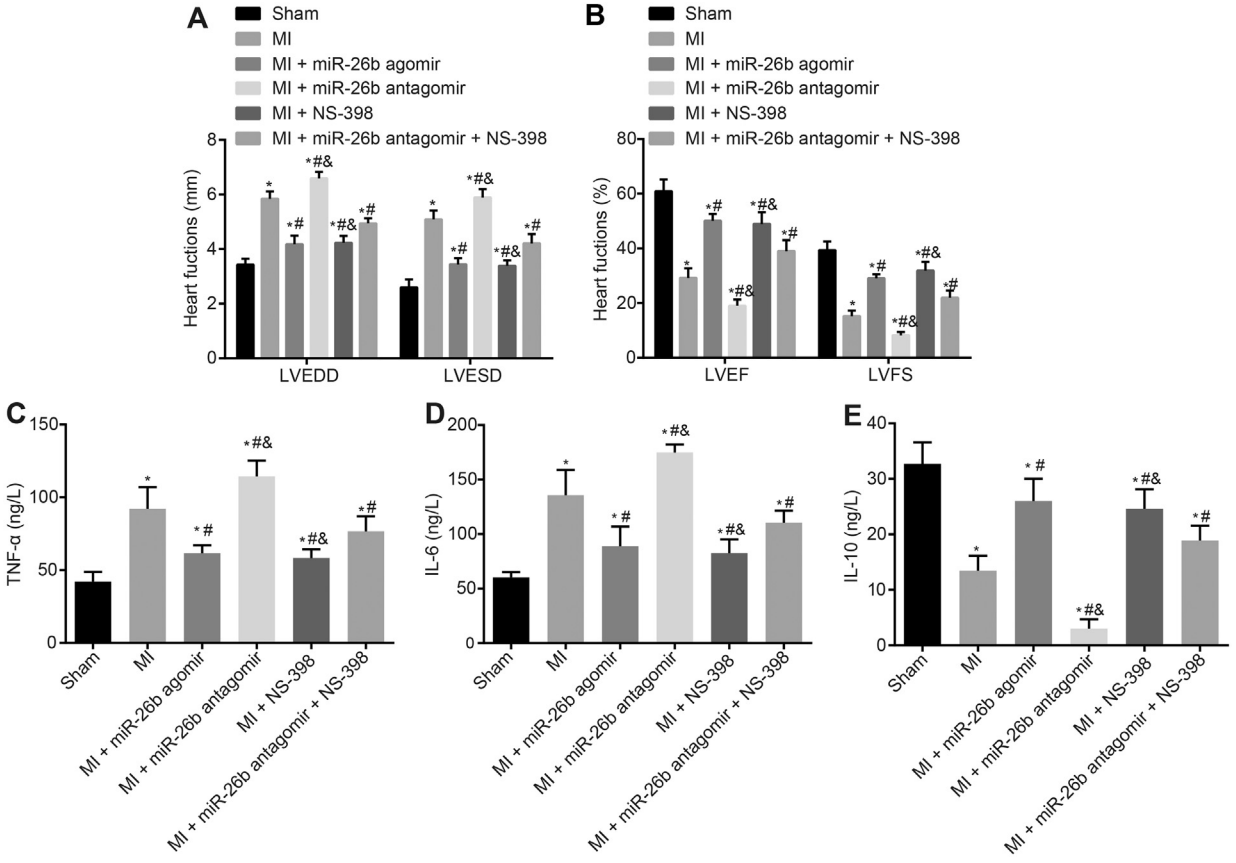

Fig. 1. Overexpressed miR-26b could improve cardiac function and alleviate the inflammatory response after MI in mice by downregulating PTGS2. A, LVEDD and LVESD of mice treated with miR-26b agomir, miR-26b antagomir and/or NS-398; B, LVFS and LVEF of mice treated with miR-26b agomir, miR-26b antagomir and/or NS-398; C, TNF-α in serum of mice treated with miR-26b agomir, miR-26b antagomir and/or NS-398; D, IL-6 in serum of mice treated with miR-26b agomir, miR-26b antagomir and/or NS-398; E, IL-10 in serum of mice in each group; *, $p < 0.05$ *vs.* the sham group; #, $p < 0.05$ *vs.* the MI group; &, $p < 0.05$ *vs.* the MI + miR-26b antagomir + NS-398 group; the experiment was repeated 3 times; data were expressed by means ± standard deviation and analyzed by one-way analysis of variance; $n = 8$.

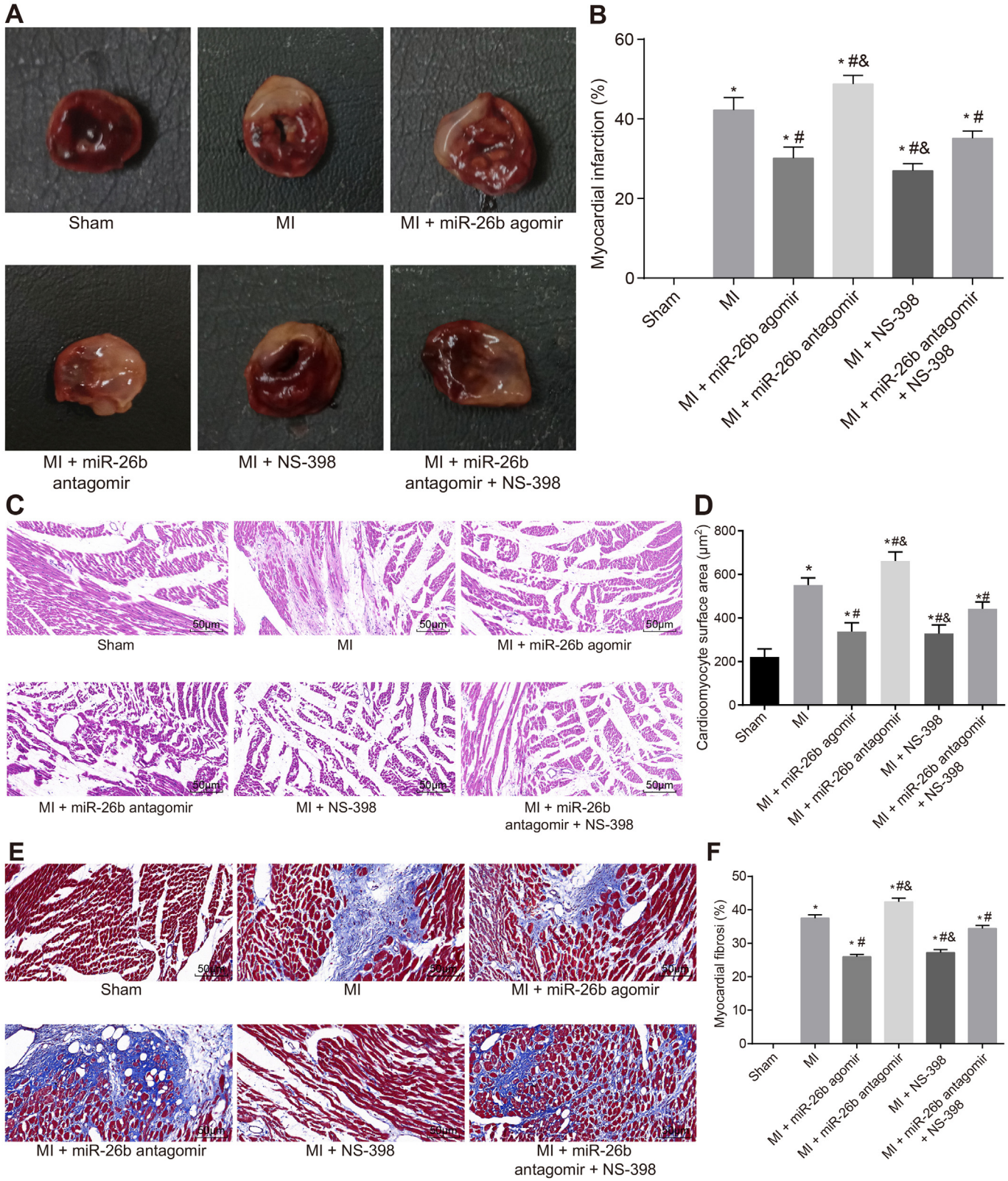

Fig. 2. Upregulation of miR-26b could reduce myocardial injury, diminish the myocardial remodeling and reduce fibrosis after MI by reducing PTGS2. A, myocardial tissues stained by TTC of mice treated with miR-26b agomir, miR-26b antagomir and/or NS-398; B, percentage of MI area of mice treated with miR-26b agomir, miR-26b antagomir and/or NS-398; C, myocardial tissues stained with HE of mice treated with miR-26b agomir, miR-26b antagomir and/or NS-398 (× 200); D, surface area of myocardial cells treated with miR-26b agomir, miR-26b antagomir and/or NS-398; E, myocardial tissues stained with Masson of mice treated with miR-26b agomir, miR-26b antagomir and/or NS-398 (× 200); F, percentage of myocardial fibrosis area; *, $p < 0.05$ *vs.* the sham group; #, $p < 0.05$ *vs.* the MI group; &, $p < 0.05$ *vs.* the MI + miR-26b antagomir + NS-398 group; the experiment was repeated 3 times; data were expressed by means ± standard deviation and analyzed by one-way analysis of variance; n = 8.

of IL-10 (Fig. 1E) on the seventh day after the MI model was built ($p < 0.05$). MI mice injected with miR-26b agomir and NS-398 showed lower expression of TNF-α and IL-6 while higher expression of IL-10 on the seventh day, while MI mice injected with miR-26b antagomir showed higher expression of TNF-α and IL-6 but lower expression of IL-10. It suggested that up-regulation of miR-26b led to the declines in the inflammatory response after MI by down-regulating the expression of PTGS2.

3.4. MiR-26b reduces myocardial injury and pathologically changes myocardial tissue as well as changes myocardial fibrosis of MI mice by downregulating PTGS2

TTC staining results showed that compared with the mice in the sham group, the mice in the MI, MI + miR-26b agomir, MI + miR-26b antagomir, MI + NS-398 group and MI + miR-26b antagomir + NS-398 groups had increased the volume of the whole heart, and their thinning left ventricular wall appeared obvious pale infarct size (Fig. 2A). Compared with the MI group, mice in the MI + miR-26b agomir group, the MI + NS-398 group and the MI + miR-26b antagomir + NS-398 group had reduced infarct size while the MI + miR-26b antagomir group had increased infarct size ($p < 0.05$). Compared with the MI + miR-26b antagomir + NS-398 group, mice in the MI + NS-398 group had reduced infarct size while the MI + miR-26b antagomir group had increased infarct size ($p < 0.05$) (Fig. 2B). All in all, the obtained results revealed that upregulated miR-26b could repress myocardial injury by downregulating PTGS2.

Compared with the mice in the sham group, the mice in the MI, MI + miR-26b agomir group, MI + miR-26b antagomir, MI + NS-398 and the MI + miR-26b antagomir + NS-398 groups increased the surface area of myocardial cells ($p < 0.05$), and their ventricular wall thickened, inflammatory cell infiltrated, cardiac muscle fibers swelled and myocardial edema appeared (Fig. 2C). Compared with the MI group, the decrease in thickening of ventricular wall, in enlargement of myocardial cell and in the surface area of myocardial cell appeared in the MI + miR-26b agomir group, the MI + NS-398 group and the MI + miR-26b antagomir + NS-398 group ($p < 0.05$) while in the MI + miR-26b antagomir group the increase in thickening of ventricular wall and in the surface area of myocardial cell, the disordered myocardial cell, hyperchromatic cytoplasm, bigger cell interval and increasing non-stained nuclei appeared ($p < 0.05$) (Fig. 2D). The aforementioned findings demonstrated that upregulated miR-26b could alleviate myocardial remodeling after MI by downregulating PTGS2.

The results of Masson staining showed that compared with the mice in the sham group, mice in the MI group, the MI + miR-26b agomir group, the MI + miR-26b antagomir group, the MI + NS-398 group and the MI + miR-26b antagomir + NS-398 group appeared the left ventricular dilatation, thinning ventricular wall and obvious pathological myocardial fibrosis (Fig. 2E). Compared with the MI group, mice in the MI + miR-26b agomir group, the MI + NS-398 group and the MI + miR-26b antagomir + NS-398 group had decreased the area of

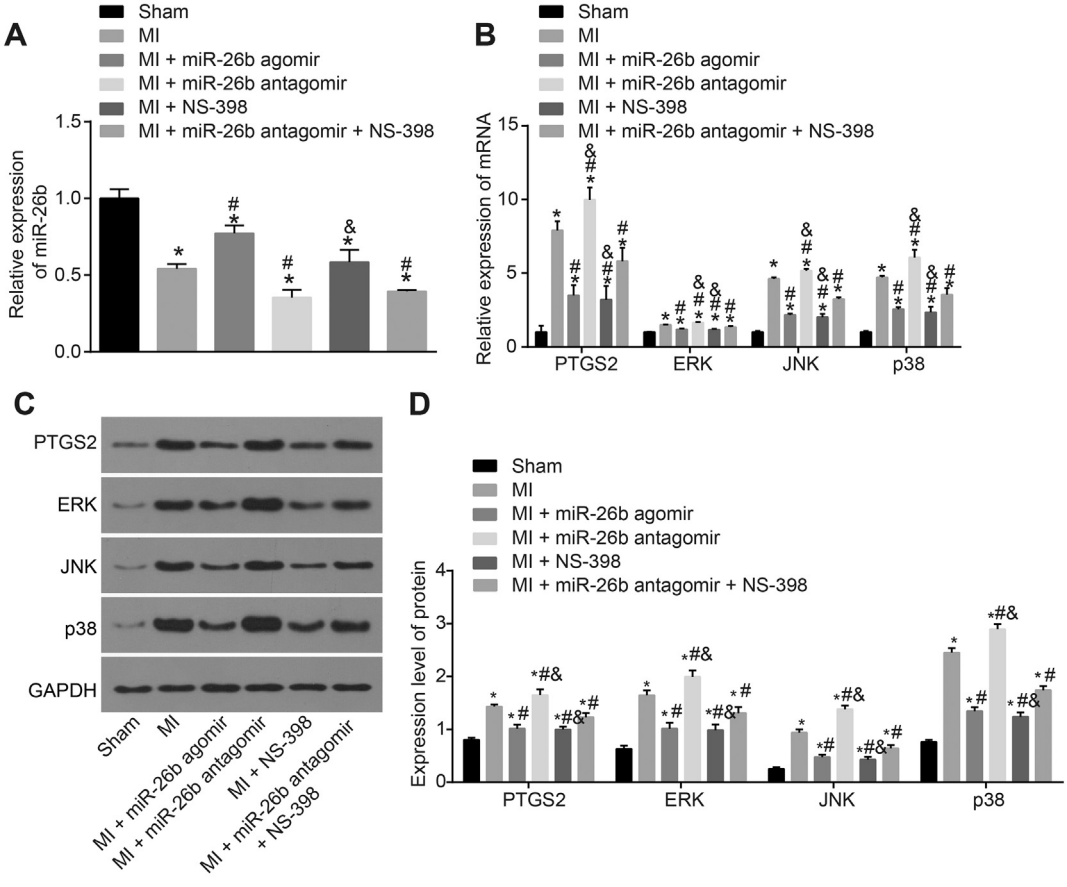

Fig. 3. Upregulation of miR-26b could inhibit activation of MAPK pathway after MI through PTGS2 downregulation. A, miR-26b expression of myocardial tissues of mice treated with miR-26b agomir, miR-26b antagomir and/or NS-398 examined by RT-qPCR; B, mRNA levels of PTGS2, ERK, JNK and p38 in myocardial tissues of mice treated with miR-26b agomir, miR-26b antagomir and/or NS-398 examined by RT-qPCR; C, the gray value of PTGS2, ERK, JNK and p38 protein bands in myocardial tissues of mice treated with miR-26b agomir, miR-26b antagomir and/or NS-398 examined by Western blot analysis; D, the protein levels of PTGS2, ERK, JNK and p38 in myocardial tissues of mice treated with miR-26b agomir, miR-26b antagomir and/or NS-398 examined by Western blot analysis; *, $p < 0.05$ *vs.* the sham group; #, $p < 0.05$ *vs.* the MI group; &, $p < 0.05$ *vs.* the MI + miR-26b antagomir + NS-398 group; the experiment was repeated 3 times; data were expressed by means ± standard deviation and analyzed by one-way analysis of variance; n = 8.

fibrosis while mice in the MI + miR-26b antagomir group had increased the area of fibrosis ($p < 0.05$). Compared with the MI + miR-26b antagomir + NS-398 group, mice in the MI + NS-398 group had decreased the area of fibrosis while mice in the MI + miR-26b antagomir group had increased the area of fibrosis ($p < 0.05$) (Fig. 2F). The aforementioned findings demonstrated that upregulated miR-26b could suppress myocardial fibrosis after MI by downregulating PTGS2.

3.5. MiR-26b inhibits the activation of MAPK pathway after MI

RT-qPCR and western blot analysis showed the higher expression of miR-26b (Fig. 3A) and lower mRNA (Fig. 3B) and protein levels (Fig. 3C-D) of PTGS2, ERK, JNK and p38 of myocardial tissues of mice in the MI group, the MI + miR-26b agomir group, the MI + miR-26b antagomir group, the MI + NS-398 group and the MI + miR-26b antagomir + NS-398 group than of the mice in the sham group ($p < 0.05$). Compared with the MI group, mice in the MI + miR-26b agomir group, the MI + NS-398 group and the MI + miR-26b antagomir + NS-398 group had decreased the mRNA and protein levels of PTGS2, ERK, JNK and p38; the mice in the MI + miR-26b antagomir group had increased mRNA and protein expression of PTGS2, ERK, JNK and p38 ($p < 0.05$). The above findings indicated that miR-26b suppressed the activation of the MAPK pathway through downregulating PTGS2.

3.6. MiR-26b inhibits myocardial cells apoptosis after MI by targeting PTGS2

The results of Western blot analysis and TUNEL staining showed that the ratio of protein level of Bcl-2/Bax (Fig. 4A-C) of mice was lower and the apoptotic index was higher in the MI group, the MI + miR-26b agomir group, the MI + miR-26b antagomir group, the MI + NS-398 group and the MI + miR-26b antagomir + NS-398 group ($p < 0.05$) (Fig. 4D–E). Compared with the MI group, mice in the MI + miR-26b agomir group, the MI + NS-398 group and the MI + miR-26b antagomir + NS-398 group had increased the ratio of protein expression of Bcl-2/Bax while decreased the apoptotic index ($p < 0.05$). The mice in the MI + miR-26b antagomir group decreased the ratio of protein expression of Bcl-2/Bax while increased the apoptotic index ($p < 0.05$). The results suggested that up-regulation of miR-26b may inhibit myocardial cell apoptosis after MI to reduce myocardial remodeling by down-regulating the expression of PTGS2.

4. Discussion

MI in humans was one of the most common cardiovascular diseases, and the increasing number of patients surviving the acute event showed the improvements in treatment for MI [27]. Also, the previous study had

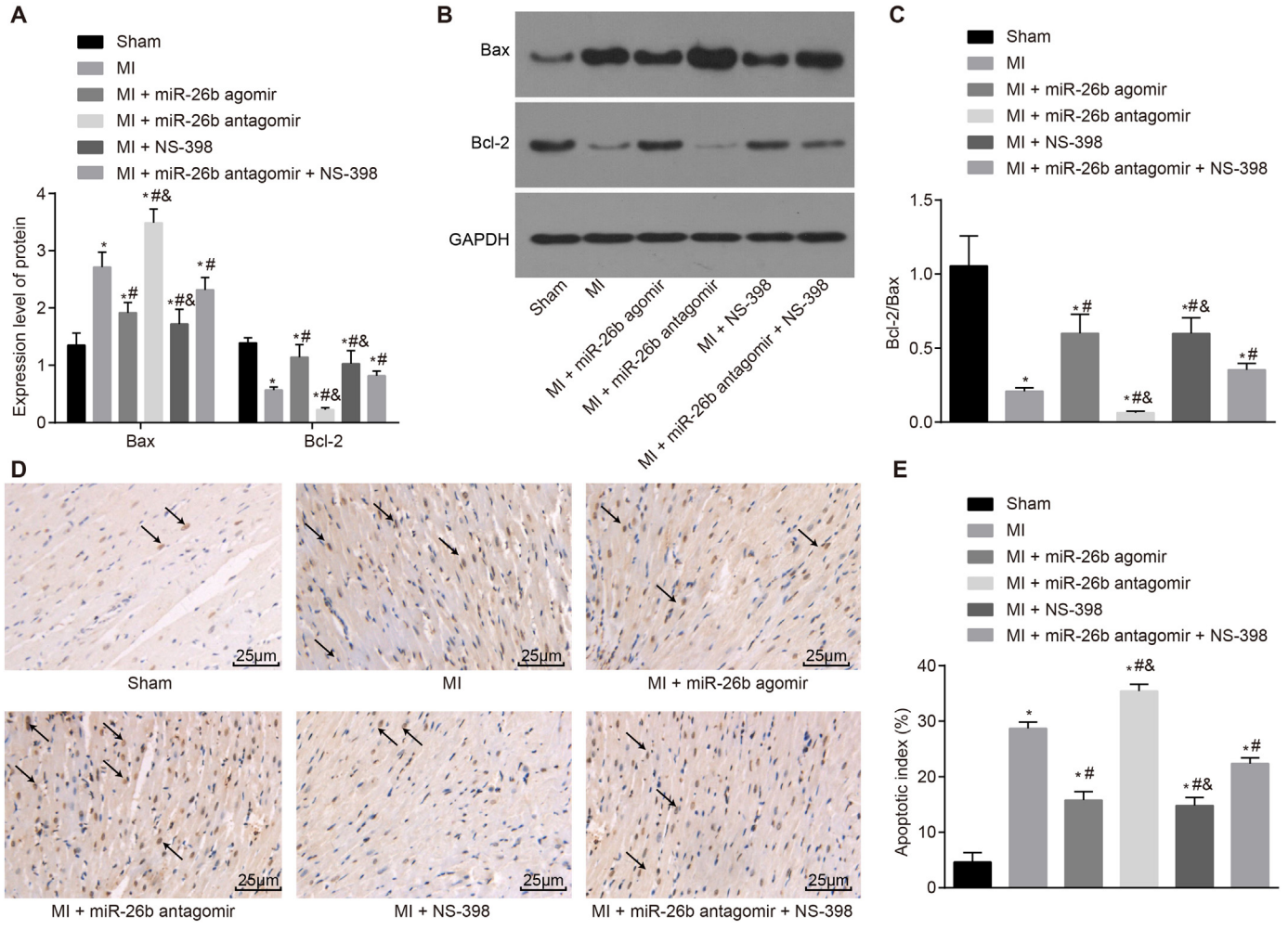

Fig. 4. Upregulation of miR-26b can inhibit myocardial cell apoptosis and alleviate myocardial remodeling after MI by reducing PTGS2 expression. A, protein levels of Bax and Bcl-2 examined by Western blot analysis; B, the gray value of Bax and Bcl-2 protein bands; C, protein level ratio between Bcl-2 and Bax; D, myocardial tissues of mice in each group stained by TUNEL (×400); E, apoptotic index of myocardial tissues of mice in each group; *, $p < 0.05$ *vs.* the sham group; #, $p < 0.05$ *vs.* the MI group; &, $p < 0.05$ *vs.* the MI + miR-26b antagomir + NS-398 group.

proved that miR-26b can function as tumor suppressors in various malignant cancers [28]. In the present study, we investigated the effect of miR-26b on mice with MI through regulating PTGS2 by MAPK pathway.

First, PTGS2 was the target gene of miR-26b and ELISA revealed that miR-26b agomir and NS-398 decreased the expression of TNF-α and IL-6 but increased the expression of IL-10, which could inhibit activation of inflammatory cells. miR-26b has been shown to directly silence PTGS2 and regulate PTGS2 expression in desferrioxamine-treated carcinoma of nasopharyngeal epithelial cells and allergic inflammation [29]. MiR-26b has been reported to have participated with the activity of inflammatory response in atrial fibrillation [30]. PTGS2 has also been confirmed to play a role in inflammatory diseases, but different from miR-26b, PTGS2 is a promotor for inflammatory response [31]. miR-26 could decrease TNF-α production so as to regulates tumourigenicity and inflammation [32]. It has been previously found that miR-26 regulated inflammation and tumorigenicity through decreasing the level of IL-6 [32]. In previous study, it was investigated that IL-10 was a synthesis inhibitory that had the ability to inhibit inflammatory cells [33] and it has been similarly indicated that the expression of IL-10 up-regulated by miRNA [34]. Additionally, myocardial remodeling was the alteration in the structure and physiological function of the heart as well as changes of cardiac cells, and previous studies had shown that many miRNAs regulated cardiac hypertrophy [35].

Additionally, we found that MAPK pathway was inhibited by upregulated miR-26b or downregulated PTGS2. Previous study has shown that MAPK pathway was likely to play an important role in pro-inflammatory responses and cell proliferation of certain tumor, and then the inhibiting effect of PTGS2 to MAPK pathway was investigated [36]. MiR-26b was studied that decreased the phosphorylation of ERK and it has also been researched relationship between the decrease of PTGS2 and regulation of MAPK pathway [37]. Previous study suggested function of PTGS2 and MAPK pathway in progression of oocyte meiosis, and then revealed inhibitory role of PTGS2 in MAPK activation [38]. A study has demonstrated activation ERK decreased because of treatments with PTGER2, a subtype of PTGS2 [39]. Here it might be inferred that miR-26b and PTGS2 contribute to inhibited activation of MAPK pathway.

Furthermore, results showed overexpressed miR-26b inhibited apoptosis of myocardial cells through suppression of MAPK pathway by binding to PTGS2. PTGS2 has been demonstrated to involve such functions as inducing apoptosis and inhibiting proliferation and suppressing metastasis [10]. In previous study, it has been confirmed the growth-suppressive effect of cells was dependent on PTGS2 [40]. Bcl-2, an anti-apoptotic factor, was demonstrated associating with PTGS2 [41]. Besides, it has been previously investigated that miR-26b-5p increased expression of Bcl-2 and decreased expression of Bax in HCC cells, suggesting inhibitory role of miR-26b- 5p on cell apoptosis [42]. In recent study, the MAPK-related factors were found to be activated in the pristine grapheme treated cells that activated pro-apoptotic member [43]. It has also been demonstrated that p38 MAPK was crucial in regulation of apoptosis and many chemotherapeutic agents demanded p38 to induce cell apoptosis [44]. From the studies above, it could be inferred that miR-26b-related mimic and PTGS2-related inhibitor had great effect in suppressing apoptosis, similarly, regulating miR-26b and PTGS2 inhibiting apoptosis of myocardial cells. Interestingly, PTGS2 inhibition has been verified to enhance mortality and left ventricular remodeling, while impedes systolic function in pig models with MI [45]. However, the study fails to provide evidence in clinical studies, and the species we chose is closer to humans.

5. Conclusion

Above all, miR-26b could inhibit inflammatory reaction and myocardial remodeling through the MAPK pathway *via* inhibiting PTGS2 expression in MI (Supplementary Fig. 3). This finding could imply that miR-26b inhibiting PTGS2 is a quite promising strategy for accelerating recovery in MI patients.

Supplementary data to this article can be found online at https://doi.org/10.1016/j.ijcard.2018.12.077.

Acknowledgements

We would like to give our sincere appreciation to the reviewers for their helpful comments on this article.

Conflicts of interest

None.

References

[1] A.S. Jaffe, F.S. Apple, The third universal definition of myocardial infarction—moving forward, Clin. Chem. 58 (2012) 1727–1728.
[2] A.E. Shafei, M.A. Ali, H.G. Ghanem, A.I. Shehata, A.A. Abdelgawad, H.R. Handal, K.A. Talaat, A.E. Ashaal, A.S. El-Shal, Mesenchymal stem cell therapy: a promising cell-based therapy for treatment of myocardial infarction, J Gene Med. 19 (2017).
[3] V. Sala, T. Crepaldi, Novel therapy for myocardial infarction: can HGF/Met be beneficial? Cell. Mol. Life Sci. 68 (2011) 1703–1717.
[4] E. Mezzaroma, S. Toldo, D. Farkas, I.M. Seropian, B.W. Van Tassell, F.N. Salloum, H.R. Kannan, A.C. Menna, N.F. Voelkel, A. Abbate, The inflammasome promotes adverse cardiac remodeling following acute myocardial infarction in the mouse, Proc. Natl. Acad. Sci. U. S. A. 108 (2011) 19725–19730.
[5] S. Zhou, L. Sun, C. Cao, P. Wu, M. Li, G. Sun, G. Fei, X. Ding, R. Wang, Hypoxia-induced microRNA-26b inhibition contributes to hypoxic pulmonary hypertension via CTGF, J. Cell. Biochem. 119 (2018) 1942–1952.
[6] D. Wang, C. Liu, Y. Wang, W. Wang, K. Wang, X. Wu, Z. Li, C. Zhao, L. Li, L. Peng, Impact of miR-26b on cardiomyocyte differentiation in P19 cells through regulating canonical/non-canonical Wnt signalling, Cell Prolif. 50 (2017).
[7] B. Icli, P. Dorbala, M.W. Feinberg, An emerging role for the miR-26 family in cardiovascular disease, Trends Cardiovasc Med 24 (2014) 241–248.
[8] Y. Kwon, Y. Kim, S. Eom, M. Kim, D. Park, H. Kim, et al., MicroRNA-26a/—26b-COX-2-MIP-2 loop regulates allergic inflammation and allergic inflammation-promoted enhanced tumorigenic and metastatic potential of Cancer cells, J. Biol. Chem. 290 (2015) 14245–14266.
[9] R.T. Gray, M.M. Cantwell, H.G. Coleman, M.B. Loughrey, P. Bankhead, S. McQuaid, et al., Evaluation of PTGS2 expression, PIK3CA mutation, aspirin use and Colon Cancer survival in a population-based cohort study, Clin. Transl. Gastroenterol. 8 (2017) e91.
[10] J. Kim, M. Shim, COX-2 inhibitor NS-398 suppresses doxorubicin-induced p53 accumulation through inhibition of ROS-mediated Jnk activation, Mol. Carcinog. 55 (2016) 2156–2167.
[11] S. Ross, J. Eikelboom, S.S. Anand, N. Eriksson, H.C. Gerstein, S. Mehta, S.J. Connolly, L. Rose, P.M. Ridker, L. Wallentin, D.I. Chasman, S. Yusuf, G. Pare, Association of cyclooxygenase-2 genetic variant with cardiovascular disease, Eur. Heart J. 35 (2014) 2242–2248a.
[12] S. Hong, S. Yu, J. Li, Y. Yin, Y. Liu, Q. Zhang, H. Guan, Y. Li, H. Xiao, MiR-20b displays tumor-suppressor functions in papillary thyroid carcinoma by regulating the MAPK/ERK signaling pathway, Thyroid 26 (2016) 1733–1743.
[13] A. Mitra, A. Ray, R. Datta, S. Sengupta, S. Sarkar, Cardioprotective role of P38 MAPK during myocardial infarction via parallel activation of alpha-crystallin B and Nrf2, J. Cell. Physiol. 229 (2014) 1272–1282.
[14] L. Gautier, L. Cope, B.M. Bolstad, R.A. Irizarry, Affy–analysis of Affymetrix GeneChip data at the probe level, Bioinformatics 20 (2004) 307–315.
[15] G.K. Smyth, Linear models and empirical bayes methods for assessing differential expression in microarray experiments, Stat. Appl. Genet. Mol. Biol. 3 (2004), 3.
[16] Y. Li, H. Zhang, H. Gong, Y. Yuan, Y. Li, C. Wang, et al., miR-182 suppresses invadopodia formation and metastasis in non-small cell lung cancer by targeting cortactin gene, J. Exp. Clin. Cancer Res. 37 (2018) 141.
[17] E. Gao, Y.H. Lei, X. Shang, Z.M. Huang, L. Zuo, M. Boucher, Q. Fan, J.K. Chuprun, X.L. Ma, W.J. Koch, A novel and efficient model of coronary artery ligation and myocardial infarction in the mouse, Circ. Res. 107 (2010) 1445–1453.
[18] W. Gong, Y. Ma, A. Li, H. Shin, S. Nie, Trimetazidine suppresses oxidative stress, inhibits MMP-2 and MMP-9 expression, and prevents cardiac rupture in mice with myocardial infarction, Cardiovasc. Ther. 36 (5) (2018) e12460.
[19] Z.X. Shen, Q.Z. Yang, C. Li, L.J. Du, X.N. Sun, Y. Liu, et al., Myeloid peroxisome proliferator-activated receptor gamma deficiency aggravates myocardial infarction in mice, Atherosclerosis 274 (2018) 199–205.
[20] E. Gao, W.J. Koch, A novel and efficient model of coronary artery ligation in the mouse, Methods Mol. Biol. 1037 (2013) 299–311.
[21] Y. Zhao, G. Huang, S. Chen, Y. Gou, Z. Dong, X. Zhang, Homocysteine aggravates cortical neural cell injury through neuronal autophagy Overactivation following rat cerebral ischemia-reperfusion, Int. J. Mol. Sci. 17 (2016).
[22] X. Wang, C. Yong, K. Yu, R. Yu, R. Zhang, L. Yu, et al., Long noncoding RNA (lncRNA) n379519 promotes cardiac fibrosis in post-infarct myocardium by targeting miR-30, Med. Sci. Monit. 24 (2018) 3958–3965.
[23] X. Loyer, V. Paradis, C. Henique, A.C. Vion, N. Colnot, C.L. Guerin, et al., Liver microRNA-21 is overexpressed in non-alcoholic steatohepatitis and contributes to the disease in experimental models by inhibiting PPARalpha expression, Gut 65 (2016) 1882–1894.

[24] Y. Zhang, J. Soto, K. Park, G. Viswanath, S. Kuwada, E.D. Abel, et al., Nuclear receptor SHP, a death receptor that targets mitochondria, induces apoptosis and inhibits tumor growth, Mol. Cell. Biol. 30 (2010) 1341–1356.
[25] M. Wang, Z. Li, X. Zhang, X. Xie, Y. Zhang, X. Wang, et al., Rosuvastatin attenuates atrial structural remodelling in rats with myocardial infarction through the inhibition of the p38 MAPK signalling pathway, Heart Lung Circ 24 (2015) 386–394.
[26] H. Yin, P. Li, F. Hu, Y. Wang, X. Chai, Y. Zhang, IL-33 attenuates cardiac remodeling following myocardial infarction via inhibition of the p38 MAPK and NF-kappaB pathways, Mol. Med. Rep. 9 (2014) 1834–1838.
[27] G.J. Strijkers, A. Bouts, W.M. Blankesteijn, T.H. Peeters, A. Vilanova, M.C. van Prooijen, H.M. Sanders, E. Heijman, K. Nicolay, Diffusion tensor imaging of left ventricular remodeling in response to myocardial infarction in the mouse, NMR Biomed. 22 (2009) 182–190.
[28] M. Li, C. Long, G. Yang, Y. Luo, H. Du, MiR-26b inhibits melanoma cell proliferation and enhances apoptosis by suppressing TRAF5-mediated MAPK activation, Biochem. Biophys. Res. Commun. 471 (2016) 361–367.
[29] J. Li, X. Kong, J. Zhang, Q. Luo, X. Li, L. Fang, MiRNA-26b inhibits proliferation by targeting PTGS2 in breast cancer, Cancer Cell Int. 13 (2013) 7.
[30] H. Zhang, L. Liu, J. Hu, L. Song, MicroRNA regulatory network revealing the mechanism of inflammation in atrial fibrillation, Med. Sci. Monit. 21 (2015) 3505–3513.
[31] J. Hellmann, Y. Tang, M.J. Zhang, T. Hai, A. Bhatnagar, S. Srivastava, M. Spite, Atf3 negatively regulates Ptgs2/Cox2 expression during acute inflammation, Prostaglandins Other Lipid Mediat. 116-117 (2015) 49–56.
[32] C.Y. Chen, J.T. Chang, Y.F. Ho, A.B. Shyu, MiR-26 down-regulates TNF-alpha/NF-kappaB signalling and IL-6 expression by silencing HMGA1 and MALT1, Nucleic Acids Res. 44 (2016) 3772–3787.
[33] C.M. Hedrich, J.H. Bream, Cell type-specific regulation of IL-10 expression in inflammation and disease, Immunol. Res. 47 (2010) 185–206.
[34] F. Ma, X. Liu, D. Li, P. Wang, N. Li, L. Lu, X. Cao, MicroRNA-466l upregulates IL-10 expression in TLR-triggered macrophages by antagonizing RNA-binding protein tristetraprolin-mediated IL-10 mRNA degradation, J. Immunol. 184 (2010) 6053–6059.
[35] Z.P. Huang, D.Z. Wang, miR-22 in cardiac remodeling and disease, Trends Cardiovasc Med. 24 (2014) 267–272.
[36] S.W. Himaya, B. Ryu, Z.J. Qian, S.K. Kim, Sea cucumber, *Stichopus japonicus* ethyl acetate fraction modulates the lipopolysaccharide induced iNOS and COX-2 via MAPK signaling pathway in murine macrophages, Environ. Toxicol. Pharmacol. 30 (2010) 68–75.
[37] K. Bhui, S. Prasad, J. George, Y. Shukla, Bromelain inhibits COX-2 expression by blocking the activation of MAPK regulated NF-kappa B against skin tumor-initiation triggering mitochondrial death pathway, Cancer Lett. 282 (2009) 167–176.
[38] F. Nuttinck, L. Gall, S. Ruffini, L. Laffont, L. Clement, P. Reinaud, P. Adenot, B. Grimard, G. Charpigny, B. Marquant-Le Guienne, PTGS2-related PGE2 affects oocyte MAPK phosphorylation and meiosis progression in cattle: late effects on early embryonic development, Biol. Reprod. 84 (2011) 1248–1257.
[39] L. Gao, B. Liu, W. Mao, R. Gao, S. Zhang, C. Fu Duritahala, Y. Shen, Y. Zhang, N. Zhang, J. Wu, Y. Deng, X. Wu, J. Cao, PTGER2 activation induces PTGS-2 and growth factor gene expression in endometrial epithelial cells of cattle, Anim. Reprod. Sci. 187 (2017) 54–63.
[40] O.J. Hickman, R.A. Smith, P. Dasgupta, S.N. Rao, S. Nayak, S. Sreenivasan, A. Vyakarnam, C. Galustian, Expression of two WFDC1/ps20 isoforms in prostate stromal cells induces paracrine apoptosis through regulation of PTGS2/COX-2, Br. J. Cancer 114 (2016) 1235–1242.
[41] S. Redondo, E. Ruiz, A. Gordillo-Moscoso, J. Navarro-Dorado, M. Ramajo, E. Rodriguez, F. Reguillo, M. Carnero, M. Casado, T. Tejerina, Overproduction of cyclo-oxygenase-2 (COX-2) is involved in the resistance to apoptosis in vascular smooth muscle cells from diabetic patients: a link between inflammation and apoptosis, Diabetologia 54 (2011) 190–199.
[42] Y. Wang, B. Sun, H. Sun, X. Zhao, X. Wang, N. Zhao, Y. Zhang, Y. Li, Q. Gu, F. Liu, B. Shao, J. An, Regulation of proliferation, angiogenesis and apoptosis in hepatocellular carcinoma by miR-26b-5p, Tumour Biol. 37 (2016) 10965–10979.
[43] Y. Li, Y. Liu, Y. Fu, T. Wei, L. Le Guyader, G. Gao, R.S. Liu, Y.Z. Chang, C. Chen, The triggering of apoptosis in macrophages by pristine graphene through the MAPK and TGF-beta signaling pathways, Biomaterials 33 (2012) 402–411.
[44] X. Sui, N. Kong, L. Ye, W. Han, J. Zhou, Q. Zhang, C. He, H. Pan, p38 and JNK MAPK pathways control the balance of apoptosis and autophagy in response to chemotherapeutic agents, Cancer Lett. 344 (2014) 174–179.
[45] L. Timmers, J.P. Sluijter, C.W. Verlaan, P. Steendijk, M.J. Cramer, M. Emons, et al., Cyclooxygenase-2 inhibition increases mortality, enhances left ventricular remodeling, and impairs systolic function after myocardial infarction in the pig, Circulation 115 (2007) 326–332.